

On the parametrization of the distributions of depth of shower maximum of ultra-high energy extensive air showers

Luan B. Arbeletche and Vitor de Souza

Instituto de Física de São Carlos, Universidade de São Paulo,

Av. Trabalhador São-carlense 400, São Carlos, Brasil.

(Dated: March 11, 2019)

Abstract

The distribution of depth in which a cosmic ray air shower reaches its maximum number of particles (X_{\max}) is studied and parametrized. Three functions are studied for proton, carbon, silicon, and iron primary particles with energies ranging from 10^{17} eV to 10^{20} eV for three hadronic interaction models: EPOS-LHC, QGSJETII.04, and SIBYLL2.3C. The function which best describes the X_{\max} distribution of a mixed composition is also studied. A very large number of simulated showers and a detailed analysis procedure were used to guarantee negligible effects of undersampling and of fitting in the final results. For the first time, a comparison of several functions is presented under the same assumption with the intention of selecting the best functional form to describe the X_{\max} distribution. The Generalized Gumbel distribution is shown to be the best option for a general description of all cases. The Log-normal distribution is also a good choice for some cases while the Exponentially Modified Gaussian distribution has shown to be the worst choice in almost all cases studied. All three functions are parametrized as a function of energy and primary mass.

I. INTRODUCTION

The relative abundance of particle compositions in ultra-high energy cosmic rays (UHECR) is of key importance in the understanding of their acceleration mechanisms and interactions with extra-galactic radiation fields. The maximum particle energy of each source, the probability of escape from the acceleration region, the luminosity of the sources classes, the mean free path of the interaction on the way to Earth and the deviation angle in the magnetic fields are examples of fundamental astrophysics phenomena which depend on the particle type (mass and/or charge). A major improvement in our understanding of UHECR physics will not be possible without a precise determination of the abundance of each particle type. With this in mind, the two most important UHECR observatories (The Pierre Auger and the Telescope Array Observatories) are implementing upgrades to enhance their capabilities to determine the relative abundances of particles arriving on Earth.

At these energies, the particles hitting Earth, called primary particles, are not directly observed. Their interaction with the atmosphere generates a cascade of particles which is measured by telescopes and ground detectors. The properties of the primary particle can be reconstructed from the detected signal of the shower. The most used and reliable parameter to determine the primary particle's type is the depth at which the cascade reaches its maximum number of particles (X_{\max}). These extensive air showers are very complex branching processes whose stochastic behavior, although well understood in terms of particle interaction processes, cannot be solved analytically. Thus, fluctuations of important global quantities such as X_{\max} have no known functional form. In this sense, one always has to rely on Monte Carlo simulations to understand the intrinsic fluctuations of extensive air showers. Moreover, an approximation to the functional form of global variables can only be determined by the parametrization of simulated quantities.

Constant improvements in the fluorescence technique have allowed the Pierre Auger Observatory to measure X_{\max} with a systematic uncertainties of about ± 8 g/cm² [1] and the TA Collaboration quotes systematic uncertainties of ± 17.4 g/cm² [2]. The resolution in $\langle X_{\max} \rangle$ are quoted to be smaller than 25 g/cm² for the Pierre Auger Observatory measurements. The precision in measuring X_{\max} is such that new studies are based on the full distribution instead of only its moments [1–5].

In this context, a good understanding of the X_{\max} distribution shape is mandatory since

many steps in the analysis procedures depend on knowing *a priori* its expected shape. Some functions have been proposed to describe the X_{\max} distribution [6, 7] but no comparison between them is available. In this paper, three functions are used to describe the X_{\max} distribution and a detailed statistical comparison between them is presented. The purpose of this paper is to select the best description of the X_{\max} distribution and parametrize its dependencies with energy and mass.

This study is based on Monte Carlo simulations of air shower which are discussed in section II. In section III, the functions used to describe the X_{\max} distribution are presented and discussed. Section IV presents the results of the fits and section VI presents the conclusions.

II. SIMULATION OF X_{\max} DISTRIBUTIONS

Large samples of extensive air showers were simulated using the software CONEX [8]. This software is an implementation of a one-dimensional hybrid model of the longitudinal development of particle cascades which has been extensively tested [6]. Four atomic nuclei were considered: proton, carbon, silicon and iron ($A = 1, 12, 28$ and 56 , respectively) with energies ranging from 10^{17} eV to 10^{20} eV in steps of 1 in $\log_{10}(E_0/\text{eV})$. The incident zenith angle of the primary cosmic rays was set to 75° . The longitudinal development was sampled in steps of 10 g/cm^2 until they reach sea level, corresponding to a slant depth of 3860 g/cm^2 . The energy cutoff for hadrons, muons, electrons, and photons is 1 GeV , 1 GeV , 1 MeV and 1 MeV , respectively. Given the known dependence on hadronic interaction models [9–11], three post-LHC hadronic interaction models were considered: EPOS-LHC [12], QGSJETII.04 [13] and SIBYLL2.3C [14]. For each combination of primary mass, energy and hadronic interaction model, 10^6 showers were simulated.

CONEX provides the depth at which a shower reaches its maximum number of particles (XMX variable in CONEX output) and the depth at which the energy deposit profile reaches its maximum (XMXDEDX in CONEX output). These variables were compared and a maximum difference of $0.8 \pm 3.4 \text{ g/cm}^2$ between them was found in all simulated cases. Given that the difference between these variables is very small, much smaller than the uncertainties of the measurements, the depth at which the shower reaches the maximum number of particles ($X_{\text{MX}}=X_{\max}$) was used in the following calculations.

X_{\max} is extracted from the simulated longitudinal profiles by fitting a quadratic function

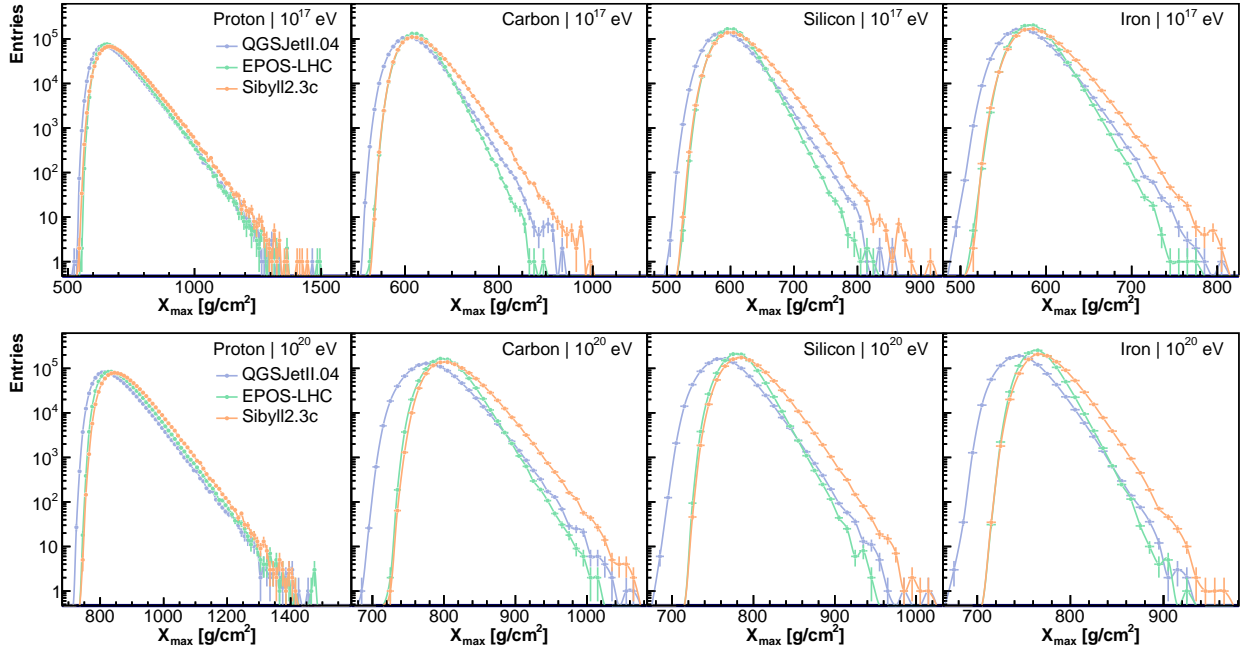


FIG. 1: Examples of simulated X_{\max} distributions for four different primary masses (Proton, Carbon, Silicon, Iron) and three hadronic interaction models (QGSJETII.04, EPOS-LHC and SIBYLL2.3C) at the energies 10^{17} eV (upper panel) and 10^{20} eV (lower panel).

around the point with the maximum number of particles. Showers with two maxima in the longitudinal profile, the so-called double bump showers [15], for which the depth of shower maximum is not an unambiguously defined quantity, are removed from our analysis. The fraction of removed profiles is below 0.4% for all combinations of primary, energy and hadronic model.

Examples of simulated X_{\max} distributions for some primary masses with energies of 10^{17} eV (upper panel) and 10^{20} eV (lower panel) are shown in figure 1. Primary types are indicated in the top-right corner of each plot. Each colored line corresponds to simulations done with a particular hadronic interaction model, indicated in the legend of the left plots. These distributions, as already known, have an accentuated positive skew that results from the exponential nature of particle interaction length distributions. Note in figure 1 the logarithm scale in the y-axis and the very small fluctuations of each point. In this illustration, X_{\max} was binned in intervals of 10 g/cm^2 . As a result from the large simulated samples, fluctuations in the obtained distributions become larger only for very deep showers.

III. PROPOSED FUNCTIONS TO DESCRIBE THE X_{MAX} DISTRIBUTIONS

In this section, three functions are studied to parametrize the X_{max} distributions: Exponentially Modified Gaussian, Generalized Gumbel, and Log-normal. They are going to be explained below and, whenever possible, an interpretation of their parameters is going to be given. The motivation for each function is also going to be briefly explored.

A. Exponentially Modified Gaussian distribution

The Exponentially Modified Gaussian (EMG) distribution was proposed in [6] to describe X_{max} distributions. It is motivated by the assumption that X_{max} can be decomposed as $X_{\text{max}} = X_{\text{first}} + \Delta X_{\text{max}}$, where X_{first} is the depth of the first interaction and ΔX_{max} represents the shower development after the first interaction. While X_{first} is known to have an exponential distribution with the mean free λ , the distribution of ΔX_{max} is unknown. The simplest approach is to assume that ΔX_{max} is normally distributed with an average μ and variance σ^2 , so that X_{max} is distributed according to the convolution of an exponential and a Gaussian. The resulting function is:

$$f(x) = \frac{1}{2\lambda} \exp\left(-\frac{x-\mu}{\lambda} + \frac{\sigma^2}{2\lambda^2}\right) \operatorname{erfc}\left(\frac{\mu-x+\sigma^2/\lambda}{\sqrt{2}\sigma}\right), \quad (1)$$

where $\operatorname{erfc}(x)$ is the complementary error function.

The EMG has three parameters that can be interpreted in terms of extensive air showers physics. λ , μ and σ are related to the decay factor of the exponential, the depth of maximum of the distribution and the width of the distribution, respectively. σ and λ influence both the width and the mean of the X_{max} distribution in different ways, mathematically $\langle X_{\text{max}} \rangle = \mu + \lambda$ and $\operatorname{RMS}(X_{\text{max}}) = \sqrt{\sigma^2 + \lambda^2}$. The EMG function has already been employed in studies such as the determination of X_{max} moments from Pierre Auger Observatory [1], the comparison between Pierre Auger Observatory and Telescope Array X_{max} data [3] and the proposal of new methods to study the mass composition from real X_{max} data [4].

B. Generalized Gumbel distribution

The Gumbel distribution arises in the field of extreme value statistics to describe the frequency of extreme events (either minimum or maximum) in series of independent and identically distributed random variables [16]. The Generalized Gumbel distribution (GMB) [17] is written as

$$f(x) = \frac{1}{\sigma} \frac{\lambda^\lambda}{\Gamma(\lambda)} \exp \left\{ -\lambda \left[\frac{x - \mu}{\sigma} + \exp \left(-\frac{x - \mu}{\sigma} \right) \right] \right\}. \quad (2)$$

Note that for $\lambda = 1$ one recovers the standard Gumbel distribution. Equation 2 was proposed by reference [7] to describe X_{\max} distributions.

The importance of the GMB distribution in extreme value statistics and its relation with the statistics of sums [18] can give some insight on its use to describe the X_{\max} distribution. Suppose a series of random variables X_k is exponentially distributed according to

$$g_k(x) = \frac{\lambda + k}{\sigma} e^{-(\lambda+k)x/\sigma}. \quad (3)$$

It has been shown in reference [19] that the sum $\sum_{k=0}^{\infty} X_k$ converges exactly to equation 2 after a convenient shift and re-scaling of X_k . That is, the asymptotic sum of exponentially distributed random variables with increasing amplitudes converges to a GMB distribution. Based on it, it is possible to interpret X_{\max} as a sum of interaction depths of multiple generations of particles, similar to the model proposed in reference [20], but with variable interaction lengths, and to write

$$X_{\max} = \sum_{k=0}^{\eta-1} X_k, \quad (4)$$

where η is the number of generations of particles. If $\eta \rightarrow \infty$ the distribution of the sum converges to equation 2. In this scenario, the mean free path of the first interaction is given by σ/λ . The scale parameter σ describes how fast the average interaction lengths change between generations of particles. The location parameter (μ) of equation 2 is introduced to shift the mean of the distribution.

For finite η , the sum above follows a beta-exponential distribution [21]:

$$f(x) = \frac{1}{\sigma B(\eta, \lambda)} e^{-\lambda x/\sigma} (1 - e^{-x/\sigma})^{\eta-1}, \quad (5)$$

where $B(x, y)$ is the beta function, defined for $x, y \geq 0$. If a location parameter (μ) is added to the beta-exponential distribution, it could as well be considered a candidate to describe X_{\max} distributions. The beta-exponential distribution was tested following the method explained below, however, it did not show any improvement in the description of X_{\max} distribution in comparison to the GMB. Since the beta-exponential function has one parameter more than the GMB, it was decided to keep only the GMB for further studies which in total has also three parameters.

C. Log-normal distribution

The log-normal distribution is characteristic of stochastic processes where the variable of interest can be written as a product of independent and identically distributed random variables so that its logarithm is normally distributed according to the central limit theorem. The log-normal distribution (LOG) proves to be difficult to interpret in terms of extensive air showers. However, as it will be shown later, it provides a good description of X_{\max} distributions. The probability density function is given by

$$f(x) = \begin{cases} 0, & \text{if } x \leq m \\ \frac{1}{\sqrt{2\pi}\sigma} \frac{1}{x-m} \exp \left\{ -\frac{[\ln(x-m)-\mu]^2}{2\sigma^2} \right\}, & \text{if } x > m. \end{cases} \quad (6)$$

It has three parameters m , μ and σ related to the position of the peak, the width of the distribution and the length of the tail, respectively.

IV. FITTING THE X_{\max} DISTRIBUTIONS

The X_{\max} distributions of each combination of primary mass, energy and hadronic interaction model were fitted using the three functions presented in the previous sections. The best description of the X_{\max} distributions was achieved by searching for the three parameters in each function which resulted in the maximum likelihood. The X_{\max} distributions were not binned (unbinned fit). The MINUIT [22] library available within the ROOT analysis framework [23] was used in the fitting procedure.

Examples of fitting results are presented in figure 2 for simulations obtained with QGSJETII.04 at an energy of 10^{20} eV. Only for illustration purposes, the distributions

were binned in intervals of 10 g/cm^2 . Note the logarithmic scale in the y-axis. The primary particle is indicated at the top-right corner of each plot. Fit functions are shown as colored solid lines, while the simulated X_{max} distribution is shown as circular dots. The bottom panels show the deviation of each fitted function to the simulated point, defined as the difference between the function and the point divided by the statistical uncertainty of the point.

Figure 2 show that the EMG distribution is not able to describe the simulated distributions for small and large X_{max} values. No clear preference between the GMB and the LOG distributions is seen.

Values of the log-likelihood for each case are shown in table I. Since the absolute value of the log-likelihood has no meaning in this unbinned fit, the values shown are relative ($\Delta\lambda_i$) to the smallest log-likelihood in each case. The first notable fact in table I is that the EMG distribution has the worst likelihood value for every primary, energy and hadronic interaction model except one: Silicon - 10^{20} eV - EPOS-LHC for which the log-likelihood value is slightly better than the GMB fit. This makes the EMG distribution the worse selection among the three functions described here to describe X_{max} distributions of single primary particles.

The GMB and LOG distributions represent similar good description of the X_{max} distributions. The LOG distribution performs better for low mass primaries (proton and carbon) and the GMB distribution performs better for heavier primaries (silicon and iron). But the differences between the quality of the fit of GMB and LOG are only marginal.

A. Mixed composition

The X_{max} distributions of events with energy between 10^{18} and 10^{19} eV measured by the Pierre Auger Observatory can be better described by a combination of primary particles rather than a pure element [5, 24]. The simulated X_{max} distributions were mixed following the fraction which best describes the Pierre Auger data as shown in reference [5] and table II. Figure 3 shows two examples of mixtures at 10^{18} eV for EPOS-LHC and SIBYLL2.3C models. Distributions were binned in intervals of 10 g/cm^2 for illustration purposes. The resulting mixture was fitted by the three proposed functions.

The $\Delta\lambda_i$ values for the fits are shown in table III. The GMB shows an overall better

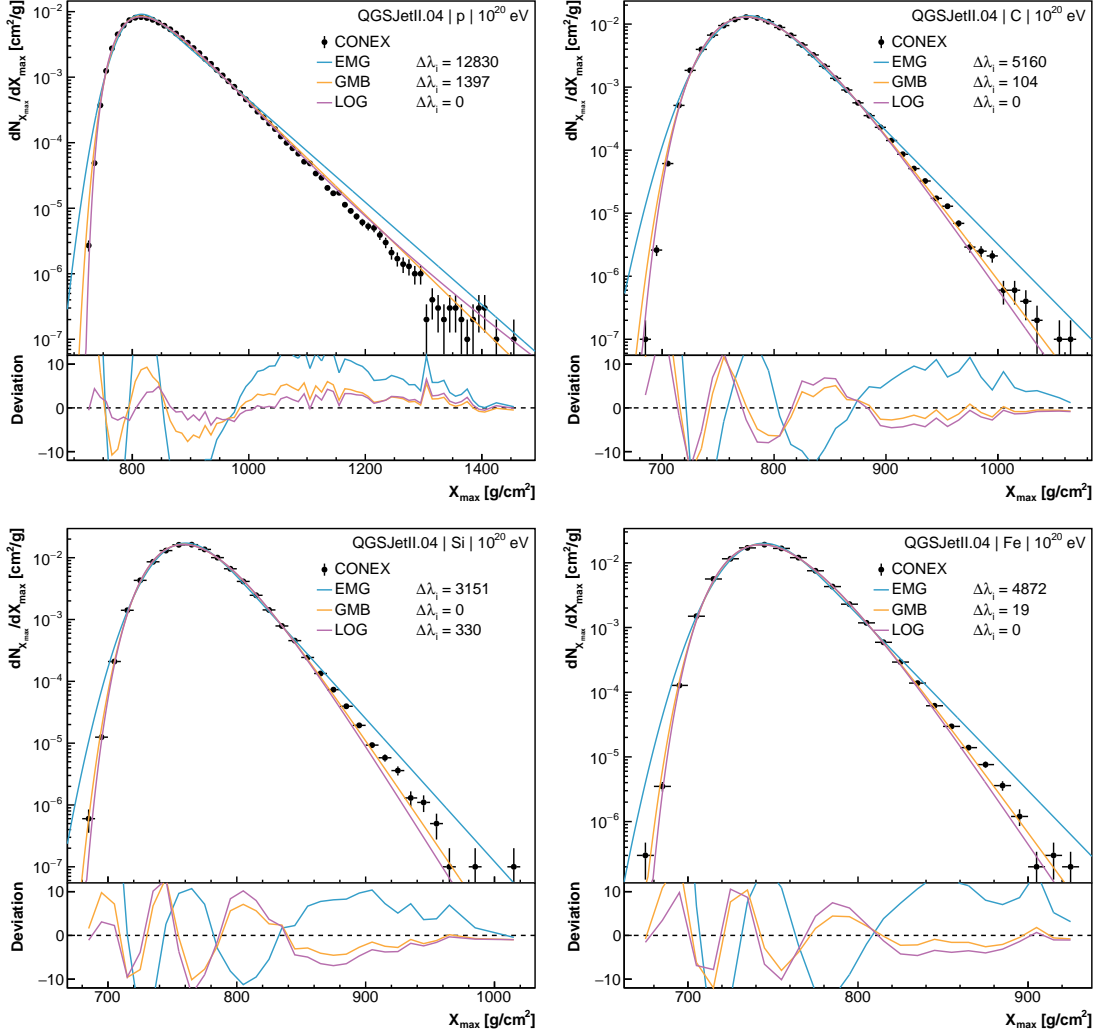


FIG. 2: Examples of fits of X_{\max} distributions. The primary particle is indicated at the top-right corner of each plot. Fit functions are shown as colored solid lines, while the simulated X_{\max} distribution is shown as circular dots. The bottom panels show the deviation of each fitted function to the simulated point, defined as the difference between the function and the point divided by the statistical uncertainty of the point. Only results for QGSJETII.04 are shown in this example.

description of the distributions, losing only marginally to the EMG for EPOS-LHC at 10^{18} eV and LOG for SIBYLL2.3C at 10^{19} eV.

QGSJETII.04																
Primary	Proton				Carbon				Silicon				Iron			
$\log(E_0/\text{eV})$	17	18	19	20	17	18	19	20	17	18	19	20	17	18	19	20
EMG	10113	11209	12226	12830	6636	6099	5181	5160	4213	3743	3447	3151	4920	5251	4875	4872
GMB	675	1044	1285	1397	131	105	32	104	0	0	0	0	0	0	0	19
LOG	0	0	0	0	0	0	0	0	402	381	384	330	202	79	81	0

EPOS-LHC																
EMG	8932	10507	13115	14264	4325	3884	3728	3027	2156	1236	1315	0	1742	1066	1571	1563
GMB	28	573	1425	1865	0	0	0	0	0	0	0	475	0	0	0	0
LOG	0	0	0	0	232	293	262	272	526	629	643	1222	681	754	781	802
EMG	8932	10507	13115	14264	4325	3884	3728	3027	2156	1236	1315	0	1742	1066	1571	1563
GMB	28	573	1425	1865	0	0	0	0	0	0	0	475	0	0	0	0
LOG	0	0	0	0	232	293	262	272	526	629	643	1222	681	754	781	802

SIBYLL2.3C																
EMG	9319	10117	11619	12648	11851	11493	11277	10987	6492	6637	6559	6269	6542	6282	5655	4954
GMB	420	666	1103	1362	914	805	760	713	0	0	0	0	0	0	0	0
LOG	0	0	0	0	0	0	0	0	247	182	123	139	326	379	495	538
EMG	9319	10117	11619	12648	11851	11493	11277	10987	6492	6637	6559	6269	6542	6282	5655	4954
GMB	420	666	1103	1362	914	805	760	713	0	0	0	0	0	0	0	0
LOG	0	0	0	0	0	0	0	0	247	182	123	139	326	379	495	538

TABLE I: Relative loglikelihood values ($\Delta\lambda_i$) of the fit of the unbinned X_{max} distributions for the three hadronic interaction models and primary particle energy ranging from 10^{17} to 10^{20} eV.

Model	EPOS-LHC		QGSJETII.04		SIBYLL2.3C	
$\log(E_0/\text{eV})$	18	19	18	19	18	19
p	61.5%	9.5%	63.2%	35.6%	40.4%	2.8%
He	0.0%	62.0%	36.8%	64.4%	9.7%	38.7%
C	36.7%	28.5%	0.0%	0.0%	49.9%	58.5%
Fe	1.8%	0.0%	0.0%	0.0%	0.0%	0.0%

TABLE II: Primary fractions which best describes the X_{max} distributions measured by the Pierre Auger Observatory [5] at the energies used in this paper.

V. PARAMETRIZATION OF X_{MAX} DISTRIBUTIONS AS A FUNCTION OF ENERGY AND MASS

The three proposed functions were used to fit the simulated X_{max} distributions for proton, carbon, silicon and iron with energies ranging from 10^{17} eV to 10^{20} eV in steps of 1 in

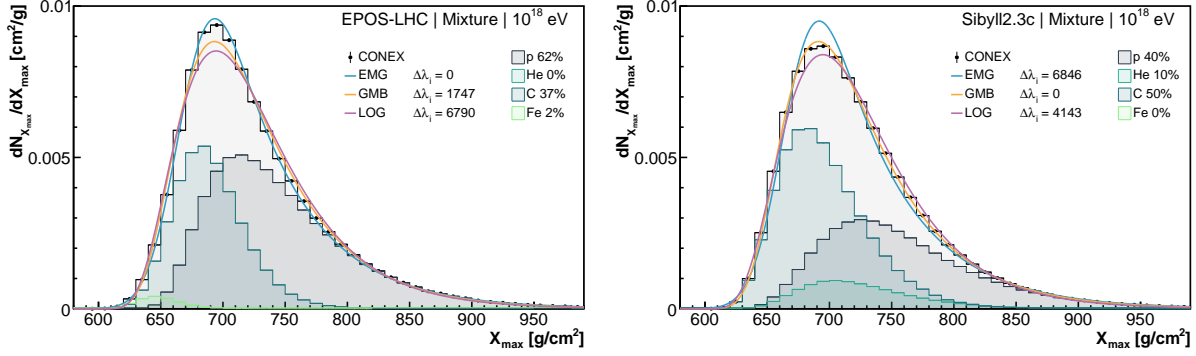


FIG. 3: Example of X_{\max} distributions at an energy of 10^{18} eV following the fractions shown in table II. Filled histograms with color lines represent the distribution of each primary particle. Black dots shows the sum of all particles. Color lines shows the result of the fit of proposed functions to the distribution of all particles (black dots). Left panel for EPOS-LHC and right panel for SIBYLL2.3C.

Model	EPOS-LHC		QGSJETII.04		SIBYLL2.3C	
	18	19	18	19	18	19
EMG	0	5557	6093	5415	6846	9378
GMB	1747	0	0	0	0	200
LOG	6790	991	4813	1457	4143	0

TABLE III: Relative loglikelihood values ($\Delta\lambda_i$) of the fit of the unbinned X_{\max} distributions for the three hadronic interaction models and mix of primary particle. Energies of 10^{18} and 10^{19} eV.

$\log_{10}(E_0/\text{eV})$. Each function has three parameters as shown in section III. These parameters were modeled as a function of primary energy and mass. The proposed functional form is:

$$\theta(E_0, A) = a(A) + b(A) \log_{10} E_0 + c(A) (\log_{10} E_0)^2, \quad (7)$$

where

$$\begin{aligned} a(A) &= a_0 + a_1 \log_{10} A + a_2 (\log_{10} A)^2, \\ b(A) &= b_0 + b_1 \log_{10} A + b_2 (\log_{10} A)^2, \\ c(A) &= c_0 + c_1 \log_{10} A + c_2 (\log_{10} A)^2. \end{aligned} \quad (8)$$

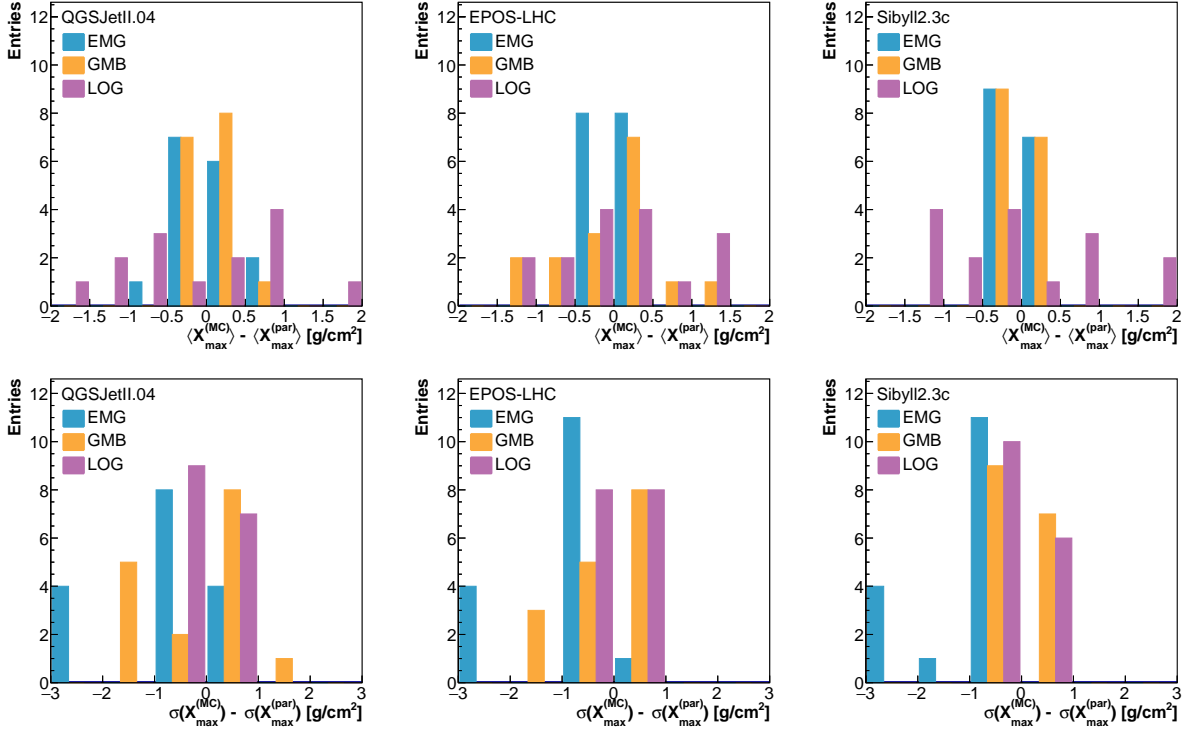


FIG. 4: Error on the first moment (upper plots) and second moment (lower plots) between the parametrized distributions (par) and the simulated (MC) X_{\max} distributions.

Values obtained for the parameters a_i , b_i and c_i are shown in table IV. Note that a value of zero in table IV means the inclusion of that parameters leads to worse fit of the simulated distribution.

The error caused by the use of equations 7 and 8 to calculate the parameters as a function of mass and energy was determined by evaluating the differences between the first and second moments of the parametrized distributions and the simulated distributions for each mass and energy. Results are shown as histograms in figure 4. The upper plots show the deviations on the first moment of the X_{\max} distributions for each hadronic interaction model indicated in the top left corner of each box. The lower plots show the differences for the second moment of the X_{\max} distributions. The largest difference between the proposed parametrization and the simulations is 2 g/cm^2 for the first moment and 3 g/cm^2 for the second moment.

VI. CONCLUSION

The X_{\max} distribution is of great importance in UHECR studies and some functional forms have been proposed to describe it. In this paper, for the first time, three functions are selected, explained, and compared to simulated X_{\max} distributions. A large sample of showers (10^6) was generated for each case in a wide range of parameters space: four atomic nuclei were considered: proton, carbon, silicon and iron with energies ranging from 10^{17} eV to 10^{20} eV and three hadronic interaction models: EPOS-LHC, QGSJETII.04, and SIBYLL2.3C. The primaries were also mixed with fractions given by the best description of the Pierre Auger Observatory data.

In total three functions were tested. Two were taken from the literature: Generalized Gumbel distribution [7] and Exponentially Modified Gaussian distribution [6] and one was proposed here: Log-normal distribution. All functions have three parameters. The parameters were fitted to the simulated X_{\max} distributions and the result is shown in table IV. The goodness of the fits allows the prediction of the first and second moments of the X_{\max} distribution with a maximum error of 2 and 3 g/cm², respectively.

The function that shows an overall best description of the X_{\max} distributions is the Generalized Gumbel distribution, followed by the Log-normal distribution. In some specific cases, the Log-normal distribution has a slightly better fit to the simulated distributions. However, in many other cases, the Generalized Gumbel distribution is much better than the Log-normal distribution. In studies of measured X_{\max} distribution, it is not possible to know beforehand which is the primary particle. Moreover, the hadronic interaction model dependence of the analysis must be minimized. For those reasons, the Generalized Gumbel distribution is proposed here as the best choice because it shows the best description for most of the cases. The Exponentially Modified Gaussian distribution is the one which most poorly describes the simulated showers among the three functions studied for almost all cases.

Acknowledgments

Authors acknowledge FAPESP Project 2015/15897-1. This study was financed in part by the Coordenação de Aperfeiçoamento de Pessoal de Nível Superior - Brasil (CAPES) -

Finance Code 001. Authors acknowledge the National Laboratory for Scientific Computing (LNCC/MCTI, Brazil) for providing HPC resources of the SDumont supercomputer (<http://sdumont.lncc.br>). Thanks to Roger Clay and Michael Unger for reading and commenting the manuscript.

- [1] A. Aab *et al.* [Pierre Auger Collaboration], Phys. Rev. D **90**, no. 12, 122005 (2014)
- [2] R. U. Abbasi *et al.* [Telescope Array Collaboration], Astrophys. J. **858**, no. 2, 76 (2018).
- [3] V. de Souza [Pierre Auger and Telescope Array Collaborations], PoS ICRC **2017**, 522 (2018).
- [4] S. Blaess, J. A. Bellido and B. R. Dawson, arXiv:1803.02520 [astro-ph.HE].
- [5] J. Bellido [Pierre Auger Collaboration], PoS ICRC **2017**, 506 (2018).
- [6] C. J. Todero Peixoto, V. de Souza and J. A. Bellido, Astropart. Phys. **47**, 18 (2013).
- [7] M. De Domenico, M. Settimo, S. Riggi and E. Bertin, JCAP **1307**, 050 (2013).
- [8] T. Bergmann *et al.* Astropart. Phys. **26**, 420-432 (2007).
- [9] R. Engel, D. Heck and T. Pierog. Annu. Rev. Nucl. Part. Sci. **61**, 467–89 (2011).
- [10] R. D. Parsons *et al.* Astropart. Phys. **34**, 832-839 (2011).
- [11] L. B. Arbeletche, V. P. Goncalves and M. A. Muller, Int. J. Mod. Phys. A **33**, no. 26, 1850153 (2018)
- [12] T. Pierog, Iu. Karpenko, J. M. Katzy, E. Yatsenko and K. Werner. Phys. Rev. C. **92**, 034906 (2015).
- [13] S. Ostapchenko. Phys. Rev. D. **83**, 014018 (2011).
- [14] A. Fedynitch, F. Riehn, R. Engel, T. K. Gaisser and T. Stanev, arXiv:1806.04140 [hep-ph].
- [15] C. Baus, R. Engel, T. Pierog, R. Ulrich and M. Unger, Proc. of 32nd ICRC.
- [16] E. J. Gumbel, Statistics of Extremes, Dover Pub. (2004).
- [17] E. Bertin, Phys. Rev. Lett. **95**, no. 17, 170601, (2005)
- [18] M. Clusel, E. Bertin, Int. J. Mod. Phys. B **22**, no. 20, 3313-3368 (2008).
- [19] T. Antal, M. Droz, G. Györgyi and Z. Rácz, Phys. Rev. Lett. **87**, no. 24, 240601, (2001)
- [20] J. Matthews, Astropart. Phys. **22**, 387 (2005).
- [21] S. Nadajarah, S. Kotz, Reliability engineering & system safety **91**, no. 6 689-697, (2006)
- [22] F. James and M. Roos, Comput. Phys. Commun. **10**, 343 (1975).
- [23] R. Brun and F. Rademakers, Nucl. Instrum. Meth. A **389**, 81 (1997).

[24] A. Aab *et al.* [Pierre Auger Collaboration], Phys. Rev. D **90**, no. 12, 122006 (2014)

Exponentially modified gaussian									
QGSJETII.04	a_0	a_1	a_2	b_0	b_1	b_2	c_0	c_1	c_2
λ	391.59	-354.39	97.214	-31.848	31.654	-9.1929	0.75259	-0.7955	0.24072
μ	-544.29	-152.02	-33.805	76.067	17.644	1.2505	-0.46924	-0.54359	0
σ	44.935	-2.6709	-4.3498	-1.033	0.25211	0	0	0	0
EPOS-LHC	a_0	a_1	a_2	b_0	b_1	b_2	c_0	c_1	c_2
λ	478.15	-576.14	204.98	-41.845	55.499	-20.799	1.0336	-1.4561	0.56255
μ	-757.99	-133.86	-32.578	99.306	15.373	0.91374	-1.053	-0.4468	0
σ	239.07	-50.644	-18.254	-23.27	7.4113	0.77829	0.624	-0.24928	0
SIBYLL2.3C	a_0	a_1	a_2	b_0	b_1	b_2	c_0	c_1	c_2
λ	389.78	-199.83	3.4634	-31.021	16.28	0.16822	0.71479	-0.39928	0
μ	-784.86	-3.3314	-15.905	100.99	-0.9832	0.43349	-1.0377	0	0
σ	80.757	8.0062	-10.197	-4.6841	-0.8151	0.52564	0.098845	0	0
Generalized Gumbel									
QGSJETII.04	a_0	a_1	a_2	b_0	b_1	b_2	c_0	c_1	c_2
λ	1.2403	11.74	-6.8456	-0.087958	-1.3926	0.85525	0.0030199	0.047022	-0.027782
μ	-368.79	-238.75	-32.141	61.443	25.159	1.2555	-0.11379	-0.73256	0
σ	55.947	20.853	-15.946	-1.0792	0.32455	0	0	0	0
EPOS-LHC	a_0	a_1	a_2	b_0	b_1	b_2	c_0	c_1	c_2
λ	4.3361	-4.8442	4.8285	-0.4489	0.42718	-0.31419	0.013249	0	0
μ	-565.11	-211.43	-36.318	82.199	22.453	1.2879	-0.61887	-0.64749	0
σ	377.32	324.05	-228.09	-37.667	-29.628	22.436	1.0216	0.73658	-0.59553
SIBYLL2.3C	a_0	a_1	a_2	b_0	b_1	b_2	c_0	c_1	c_2
λ	0.022155	0.15902	0.10957	0.038498	0.013524	0	0	0	0
μ	-537.61	-131.99	-19.675	78.952	11.515	0.73123	-0.4886	-0.33658	0
σ	59.996	23.994	-16.746	-1.0612	-1.5034	0.78286	0	0	0
Log-normal									
QGSJETII.04	a_0	a_1	a_2	b_0	b_1	b_2	c_0	c_1	c_2
μ	8.9738	-0.83993	0.31659	-0.39776	0.068381	-0.034365	0.0096036	0	0
σ	0.53182	-0.076799	-0.039262	-0.0064559	-0.0098711	0.006566	0	0	0
m	-1152.4	64.852	-50.044	129.78	-8.739	4.6464	-1.8465	0	0
EPOS-LHC	a_0	a_1	a_2	b_0	b_1	b_2	c_0	c_1	c_2
μ	14.745	-2.0402	0.043066	-1.058	0.27607	-0.02296	0.028065	-0.0075181	0
σ	0.033857	-0.31017	0.004327	0.054352	-0.0010422	0.0058172	-0.0017682	0	0
m	-1745.1	-168.59	23.864	198.41	4.0434	0.64396	-3.7383	0	0
SIBYLL2.3C	a_0	a_1	a_2	b_0	b_1	b_2	c_0	c_1	c_2
μ	5.7822	-0.026644	-0.059285	-0.042226	-0.0093557	0	0	0	0
σ	0.55075	-0.15136	0.013976	-0.0086094	0.0025617	0	0	0	0
m	-1085.3	-66.408	24.162	120.33	2.6809	-1.3847	-1.4934	0	0

TABLE IV: Parametrization of X_{\max} distributions as a function of primary energy and mass.